Available online at www.sciencedirect.com

SciVerse ScienceDirect

Ceramics International 39 (2013) 1893–1899

CERAMICS INTERNATIONAL

www.elsevier.com/locate/ceramint

Effect of PMMA pore former on microstructure and mechanical properties of vitrified bond CBN grinding wheels

Xingfen Lv, Zhihong Li*, Yumei Zhu, Jiashuo Zhao, Guangtao Zhao

Key Laboratory for Advanced Ceramics and Machining Technology of Ministry of Education, School of Materials Science and Engineering, Tianjin University, Tianjin 300072, People's Republic of China

Received 21 June 2012; received in revised form 23 July 2012; accepted 12 August 2012
Available online 18 August 2012

Abstract

Vitrified bond cubic boron nitride (CBN) grinding wheels with various porosities (36.5–43.5%) were fabricated by adding polymethylmethacrylate (PMMA) and activated carbon pore former. The effects of the type and content of pore formers as well as the size of PMMA on final porosity, microstructure and mechanical properties were investigated. PMMA was confirmed to be a more appropriate pore former for vitrified bond CBN grinding wheels than activated carbon. The porous specimens prepared with PMMA demonstrated quasi-spherical pores with more uniform pore size distribution, and higher bending strength and hardness than those prepared with activated carbon. The higher content of pore former led to increased porosity of sintered specimens, resulting in a decrease in the bending strength and hardness. Furthermore, as the size of PMMA increased, the total porosity remained almost unchanged, while the bending strength and hardness decreased firstly and then increased. Observations carried out by scanning electron microscope (SEM) and optical microscope showed that the size and shape of pores produced by PMMA were related to those of the initial PMMA microspheres, so that good control of pore size and microstructure could be obtained in vitrified bond CBN grinding wheels.

Keywords: B. Porosity; C. Mechanical properties; PMMA; Microstructure

1. Introduction

Vitrified bond cubic boron nitride (CBN) grinding wheel is one of the most promising abrasive tools because of the outstanding properties such as high material removal rates, high heat resistance, good self-sharpening, easy dressing, long wheel life, low total cost and so on [1,2]. It has been widely used in various types of grinding operations for metallic materials such as steel, cast iron and superalloy, ranging from high efficiency grinding to high precision grinding [3–6]. In comparison with metal and resin bond CBN grinding tools, vitrified bond CBN grinding tools show higher bond strength and more excellent self-dressing capability. Furthermore, a certain number of pores with different sizes can be introduced into the grinding wheel for vitrified bond ones [7–9]. On account of the high elastic modulus and low fracture toughness of the glass bonding materials, properly designed pores distributed between the bond bridges can restrain crack propagation and increase the impact strength of vitrified bond grinding wheels. In addition, such a structural possibly can reduce the frictional heat generated during grinding by reducing the contact area and by allowing the flow of cooling fluid in the pores, which is conducive to improving the surface quality of the work pieces and the grinding efficiency of grinding wheels as well as the service life. However, when the porosity increases further, the strength of the bond bridges and carrying load area decreases, leading to a decline both in the mechanical properties and grinding properties of the wheels [10,11]. Therefore, it is crucial to control the porosity and morphology of pores for vitrified bond grinding wheels to yield optimized combination of the mechanical strength, hardness, grinding efficiency, service life and surface finish of the work pieces.

*Corresponding author. Tel./fax: +86 022 27404260.
E-mail address: zhlitju@yahoo.cn (Z. Li).

0272-8842/$ - see front matter © 2012 Elsevier Ltd and Techna Group S.r.l. All rights reserved.
http://dx.doi.org/10.1016/j.ceramint.2012.08.038

It has been reported that there are two major categories of processes to obtain high porosity abrasive tools [12]. The first category is the burn-out method, where pore structure is produced by addition of organic pore inducing media (such as walnut shells, spherical polymers) in mixing stage. These media thermally decompose upon firing of the green body, leaving voids or pores in the cured abrasive tool. The second category is the bubble method, by introducing materials such as bubble alumina into the abrasive tool. Owing to their relatively high melting point, the bubble materials are not burnt out after sintering, thus the closed pores appear in the abrasive tool. While grinding, their outer surfaces disintegrate, thus forming additional cutting edges and their empty interiors become temporary shallow chip stores [13]. Polymethylmethacrylate (PMMA) microsphere, a kind of spherical polymer that can be easily burned out, is often used as the pore former of porous ceramics and solid oxide fuel cells [14–18], while it is rarely applied to vitrified bond grinding wheels. In this work, vitrified bond CBN grinding wheels using PMMA microsphere as the pore former were prepared. The pore-forming effects of PMMA microsphere and activated carbon were compared in terms of the porosity, pore morphology and mechanical properties of grinding wheels. Additionally, the porosity, microstructure and mechanical properties of vitrified bond CBN grinding wheels as a function of the content and the size of PMMA pore former were also investigated.

2. Experimental procedures

The pre-fritted glass binder composed of 52.0 wt% SiO_2–19.5 wt% B_2O_3–11.5 wt% Al_2O_3–6.4 wt% Na_2O–5.8 wt% K_2O–4.8 wt% BaO was used in this study. Polymethylmethacrylate (PMMA, Beijing Athanasy Technology Development Co., Ltd., China) and activated carbon (Tianjin University Kewei New Material Technology Development Co., China) were used as pore formers. The compositions of specimens investigated in this study are shown in Table 1, with the mass fraction of the pore former being the main variable. The particle sizes of PMMA microspheres used in this study are presented in Table 2. CBN grains (monocrystal, 325/400 mesh, Henan Funik Ultrahard Material Co. Ltd., China), Al_2O_3 fillers, and glass binder were homogeneously mixed with the pore former at various contents. The mass ratio of CBN, Al_2O_3 and glass binder was always 1: 4: 2.5. Temporary adhesive (paraffin wax) was subsequently added and mixed with the powder at about 80 °C. Then the granules formed by sieving the mixture with a screen were pressed into rectangular bars ($30.0 \times 6.0 \times 4.0$ mm) and cylinder specimens ($\Phi 15.0 \times 10.0$ mm) at 100 MPa and 125 MPa, respectively. The green specimens were sintered in an electric furnace in air. They were firstly heated to 250 °C at the rate of 3 °C/min, held for 30 min for elimination of humidity and burnout of temporary adhesive, afterwards heated to 720 °C at the rate of 1 °C/min, held for 30 min for the removal of the pore former, and then heated to 840 °C at 3 °C/min, held for 120 min, at last, furnace-cooled to the room temperature.

The decomposition or combustion temperature of the pore formers was ascertained by thermogravimetric analysis (TGA) using simultaneous thermal analyzer (Netsch STA 449C, Germany) with the heating rate of 10 K/min in air atmosphere. The porosity of each sintered specimen was determined by the Archimedes method using distilled water as medium. The bending strength was measured by a universal testing machine (XWW, Beijing Jinshengxin Detecting Instrument Co., Ltd., China) with a cross-head speed of 0.6 mm/min. The hardness was performed via Rockwell hardness tester (HR-150A). The average hardness of 10 measurement positions on the surface of each cylinder specimen was recorded. Every three specimens as a group were taken to the measurements to obtain the average value of porosity, bending strength and hardness, respectively. Rectangular bars were tested to obtain the average value of porosity and bending strength, while cylinder specimens were tested to obtain the average hardness. The microscopic morphology of specimens was observed by optical microscope (OLYMPUS-BX51M) and scanning electron microscope (SEM, S-4800, Hitachi Ltd., Japan).

Table 2
Particle sizes of PMMA microspheres used in this study (specifications from supplier).

Specimens	Average particle size of PMMA (μm)	Standard deviation
G4-7	7	1.41
G4-10	10	2.71
G4-15	15	2.03
G4-20	20	2.76
G4-60	60	6.28

Table 1
Compositions of specimens investigated in this study.

Specimens	CBN (wt%)	Al_2O_3 (wt%)	Glass binder (wt%)	Temporary adhesive (wt%)	Pore former (wt%)
G0	14.2	57.0	22.8	6	0
G2	13.9	55.8	22.3	6	2
G4	13.6	54.6	21.8	6	4
G6	13.3	53.4	21.3	6	6
G8	13.0	52.2	20.8	6	8

3. Results and discussion

3.1. Characteristics of pore formers

The combustion or decomposition behavior of the pore formers was carried out by thermogravimetric analysis (TGA) to determine the optimum heating procedure. Fig. 1 shows the TG curves of activated carbon and PMMA in air atmosphere, respectively. The main weight loss of activated carbon occurred between 360 °C and 720 °C, indicating that the activated carbon was oxidized up to 360 °C and was completely combusted at about 720 °C. In comparison with the activated carbon, PMMA decomposed rapidly at lower temperatures ranging from 250 °C to 400 °C, and the burn-out of PMMA was more completed in the testing temperature region. To assure the completeness of burn-out of pore former and avoid cracking and "blackening" of the fired specimens, the heating rate of the green samples was set at 1 °C/min during the sintering temperature from 250 °C to 720 °C.

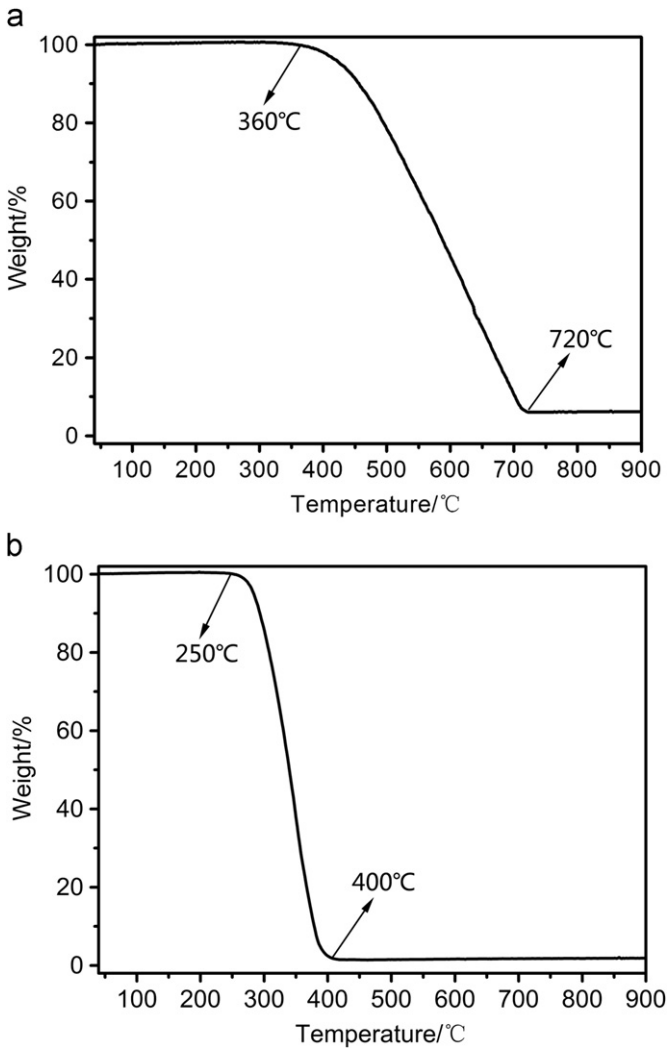

Fig. 1. TG curves of pore formers: (a) activated carbon and (b) PMMA.

Particle morphology of the two kinds of pore formers is exhibited in Fig. 2. Activated carbon contained many angular particles with various sizes ranging from 3 μm to 30 μm. They had rough surface and micro-porous structure and the larger particles appeared to be the agglomeration of smaller ones. In Fig. 2(b), PMMA microspheres obviously had spherical structure with smooth surface, whose average particle size was 7 μm in diameter.

3.2. Effect of the type and content of pore formers on the performance of vitrified bond CBN grinding wheels

Fig. 3 shows the fracture surface micrographs of specimens prepared with various contents of PMMA and activated carbon, respectively. It was obvious that the microstructures were gravely affected by the amount and type of pore former. In Fig. 3(a), the specimen prepared without any pore formers did present a porous microstructure. A number of irregular pores and some small, close pores could be observed. Since the vitrified bond was fritted in advance, there was no gas generated by the chemical reaction of pre-fitted glass. Thus, the pores were mainly derived from the gaps remaining in the green body when the vitreous grains and abrasive particles

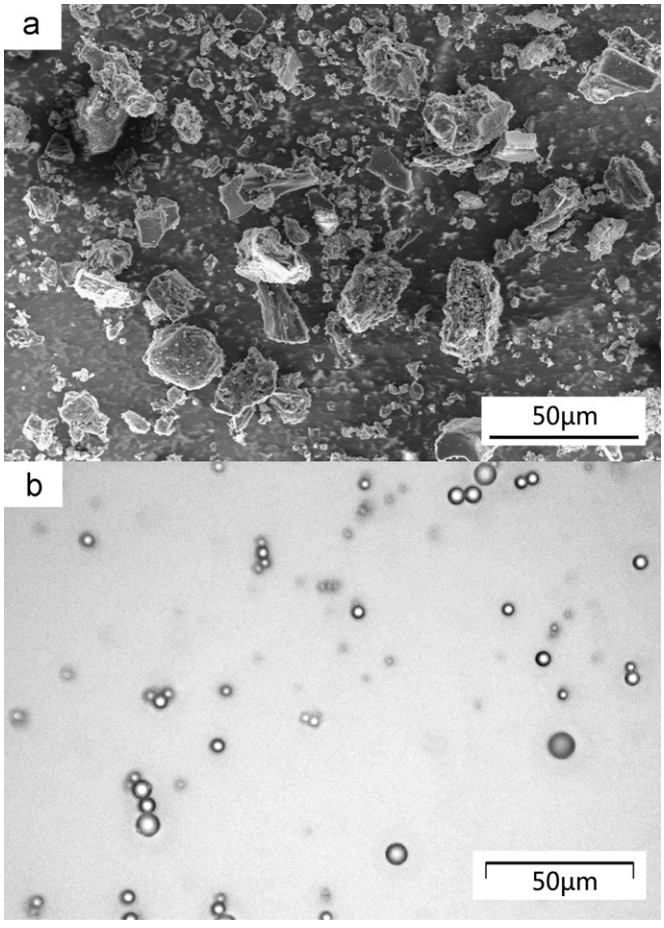

Fig. 2. Particle morphology of the pore formers: (a) activated carbon through SEM and (b) PMMA microspheres through optical microscope.

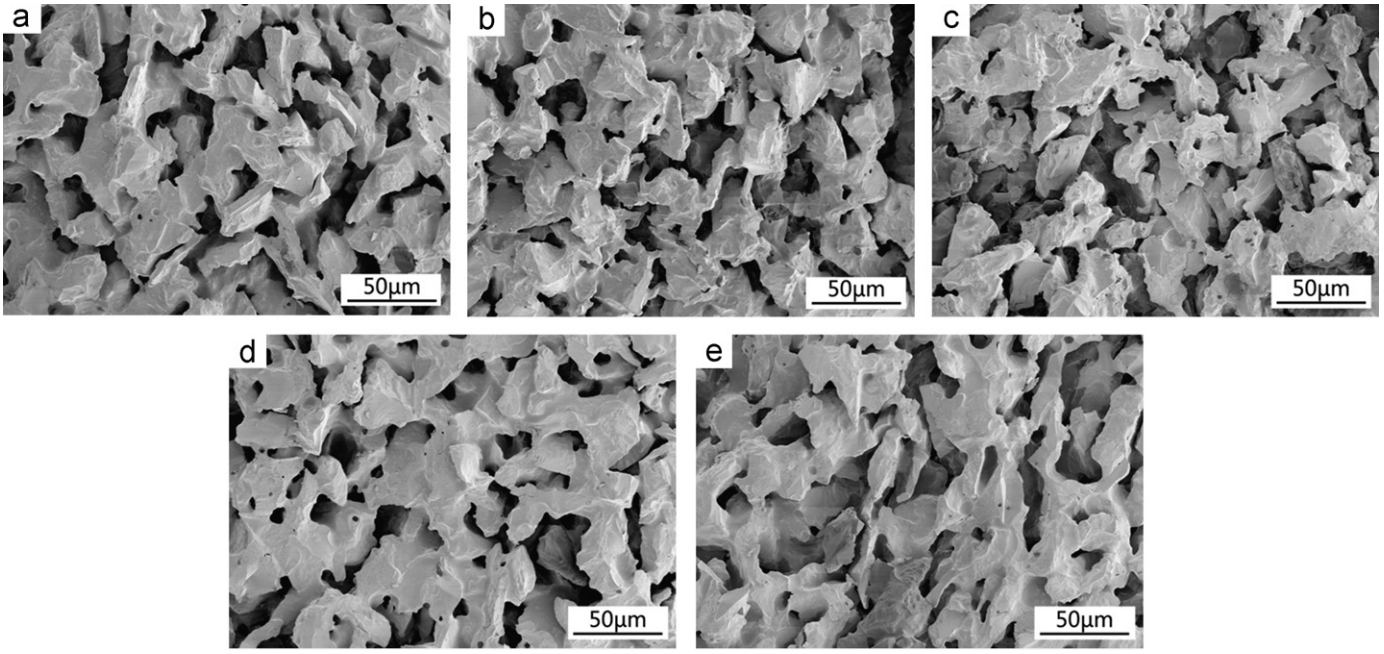

Fig. 3. SEM micrographs of specimens prepared with various contents of pore formers: (a) no pore former, (b) 4 wt% activated carbon, (c) 8 wt% activated carbon, (d) 4 wt% PMMA and (e) 8 wt% PMMA.

agglomerated together in the process of sintering. As the content of the pore former increased, the total volume and connectivity of pores increased, as well as the pore size. On the other hand, the material prepared with activated carbon showed a mass of irregular pores with various sizes. By contrast, the material made with the same content of PMMA had relatively small quasi-spherical pores between 5 and 10 μm in diameter, and the pores formed by PMMA were more uniform in distribution than those by activated carbon as shown in Fig. 3(b)–(e). However, some pores inside were deformed as exhibited in Fig. 3(d). This probably because the fluid glass flowed at high temperature, when PMMA had decomposed completely, resulting in slumping of the thin wall of pore. In general, both kinds of pores in the specimens were similar in shape to the pore formers themselves (Fig. 1), indicating that the morphology of the pores was related to the shapes and sizes of the initial pore formers, as has already been demonstrated in the literature [19,20].

Fig. 4 shows the porosity, bending strength and Rockwell hardness of specimens prepared with various pore formers. It can be seen that the porosity of specimens increased, the bending strength and Rockwell hardness decreased with an increase in the content of the pore former, independent of the type of pore former used. Additionally, the bending strength and Rockwell hardness of specimens prepared with PMMA were obviously higher than those of specimens prepared with activated carbon, while the porosity of the former was negligibly lower than the latter in the same conditions. As shown in Fig. 4(a), the porosity increased almost linearly with the content of pore former in the range of testing. When the content of the pore former increased from 0 wt% to 8 wt%, the porosity of specimens increased from 36.5% to around 43.5%. In Fig. 4(b), the bending strength of specimens dropped from approximately 90 MPa to 59.7 MPa when the PMMA content increased from 0 wt% to 8 wt%, while the bending strength dramatically decreased to 38.6 MPa for specimens adding 8 wt% activated carbon. The variations of Rockwell hardness were similar to the bending strength, but when adding 8 wt% activated carbon, the Rockwell hardness of specimens was too low to measure, as illustrated in Fig. 4(c).

These results were consistent with previous correlational studies that the mechanical strength of the specimen was conversely relative to the content of pore former and final porosity [21–23]. This was due to that the addition of the pore former into specimens inevitably improved the porosity of the specimens and reduced the sturdiness of the bond bridges between adjacent particles of abrasive, which could significantly decrease the bending strength of specimens. The changing trend of Rockwell hardness was somewhat similar to that of the bending strength because the hardness of a grinding wheel was directly influenced by the strength of the bonding at the grain and the strength of the bond bridges. On the other hand, the specimens prepared with PMMA attained a sintered structure of better mechanical properties than those with activated carbon under the same conditions. This occurred probably due to relatively visible deficiency such as irregular pores with various sizes yielded in the specimens prepared with activated carbon. It was more likely to cause stress concentration at the defect tip and make the grinding wheel suffer cracking and tearing in the presence of

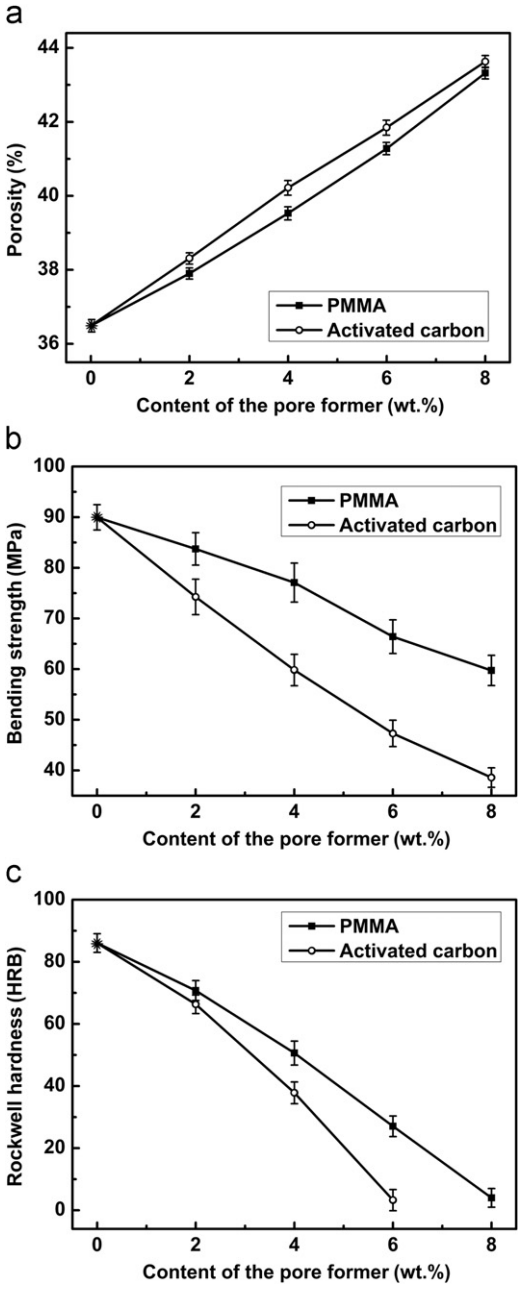

Fig. 4. Variations of (a) porosity, (b) bending strength and (c) Rockwell hardness of specimens with the content of PMMA and activated carbon, respectively.

external forces, leading to deterioration of the mechanical properties [24]. Comparing the pore-forming effects of activated carbon and PMMA microspheres, it was clearly concluded that the introduction of PMMA pore former could produce quasi-spherical pores with relatively uniform pore size distribution, and had a less influence on impairing the strength and hardness than activated carbon. So PMMA pore former adjusted the porosity more effectively on the premise of ensuring the strength and hardness of vitrified bond CBN grinding wheels at an acceptable level so as to guarantee wheel safety and life.

3.3. Effect of the size of PMMA on the performance of vitrified bond CBN grinding wheels

The effect of the size of PMMA was investigated for specimens listed in Table 2. Fig. 5 exhibits the fracture surface micrographs of specimens adding 4 wt% PMMA with various sizes, along with optical images of the pore formers themselves. There were two types of pores in the specimens. One was the irregular pores derived from the gaps remaining in the green body during sintering as mentioned above. The other was the quasi-spherical pores created by the decomposition of PMMA. It was shown that the quasi-spherical pore dimensions distinctly changed with the PMMA size used in the preparation of the grinding wheel. As the PMMA particle size increased, fewer quasi-spherical pores with larger sizes were uniformly distributed in the specimens. Such an observation indicated that the quasi-spherical pore dimensions corresponded with the particle size of the PMMA. Therefore, the pore size distribution can be controlled by adding different sizes of PMMA into vitrified bond CBN grinding wheels.

Fig. 6 shows the effects of different sizes of PMMA on the porosity, bending strength and Rockwell hardness of vitrified bond CBN grinding wheels. With an increase in the size of PMMA, there was no obvious change in total porosity, for the content of PMMA was constant. However, the Rockwell hardness and bending strength decreased firstly and then increased as the PMMA size increased, reaching the minimum value at an average size of 15 μm. This was probably related to the sizes and spatial distributions of pores in materials. By SEM, we could find that the small pores formed by PMMA were mainly surrounded by the vitrified bond. As the pore size increased, the pores began to be bounded by several abrasive grains and the spherical pores became seriously distorted. The presence of irregularly shaped and relatively large pores within the materials could significantly reduce the sturdiness of the bond bridges, resulting in the rapid deterioration of the bending strength and hardness of specimens. When the pores became much larger, they were encircled by multiple abrasive grains and bond bridges, but the spherical pores were slightly deformed. On the other hand, with the enlargement of PMMA grain size from 15 μm to 60 μm, the number of the spherical pores in specimens fell markedly, which had a positive effect upon the mechanical strength of the materials. Therefore, compared with the specimens containing a mass of small and irregularly shaped pores, the materials with a small number of large spherical pores ultimately presented higher bending strength and hardness.

4. Conclusions

Vitrified bond CBN grinding wheels with various porosities (36.5–43.5%) have been manufactured by using different pore formers (PMMA, activated carbon). The higher

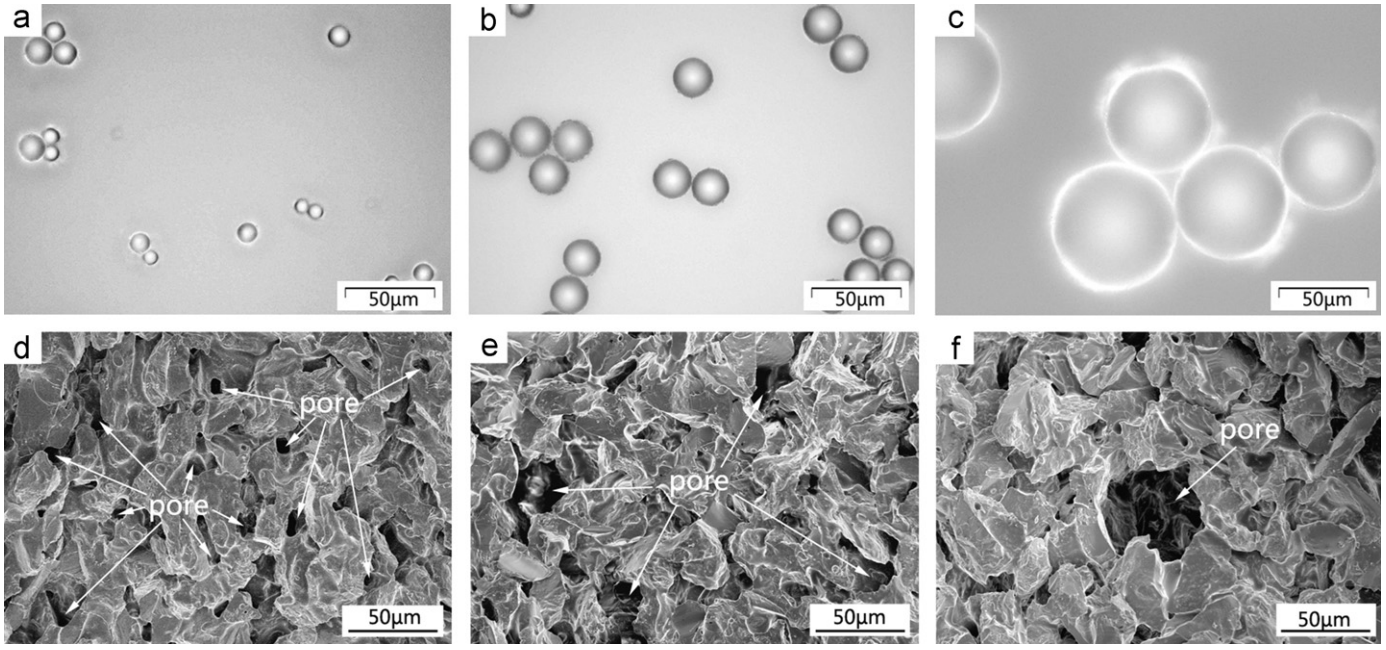

Fig. 5. (a–c) Optical images of various sizes of PMMA: (a) 10 μm, (b) 20 μm, (c) 60 μm. (d–f) SEM micrographs of specimens adding 4 wt% PMMA with various sizes: (d) G4-10, (e) G4-20 and (f) G4-60.

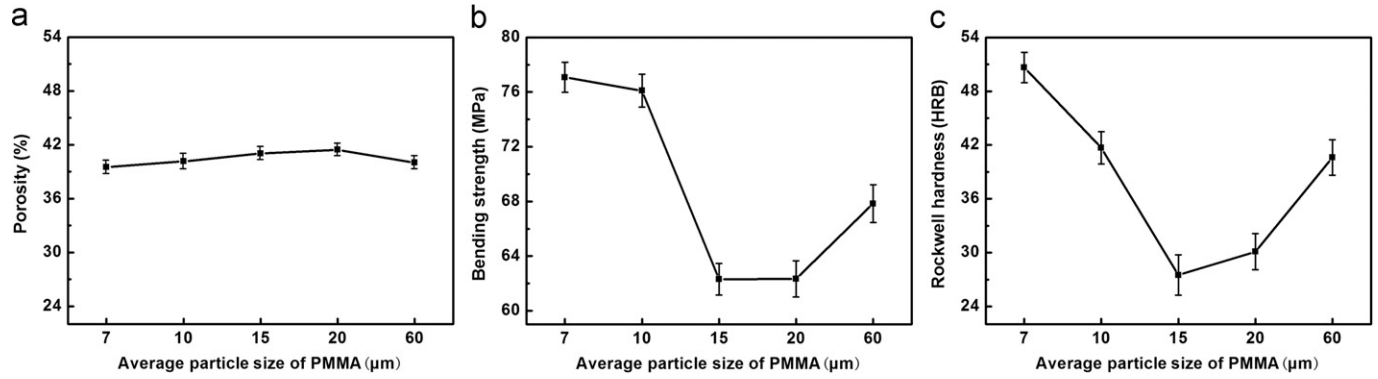

Fig. 6. Variations of (a) porosity, (b) bending strength and (c) Rockwell hardness of specimens with the size of PMMA.

content of pore formers caused a rise in porosity and a drop in both bending strength and hardness, independent of the type of pore former used. Compared with activated carbon, PMMA pore former produced quasi-spherical pores with relatively uniform pore size distribution, and had a less influence on impairing the strength and hardness. Hence, PMMA was an appropriate pore former for vitrified bond CBN grinding wheels better than activated carbon. In addition, with an increase in the size of PMMA, there was no obvious change in total porosity, while the bending strength and hardness decreased firstly and then increased. SEM and optical microscope observation revealed that the morphology of the pores produced by PMMA was related to the shapes and sizes of the PMMA microspheres, so the pore size and microstructure could be successfully controlled by adding PMMA pore former into vitrified bond CBN grinding wheels.

References

[1] M.J. Jackson, Sintering and vitrification heat treatment of CBN grinding wheels, Journal of Materials Processing Technology 191 (2007) 232–234.
[2] I.D. Marinescu, W.B. Rowe, B. Dimitro, in: Tribology of Abrasive Machining Processes, William Andrew, New York, 2004.
[3] N. Funayama, J. Matsuda, Development of high-performance CBN and diamond grinding wheels for high-speed grinding, New Diamond and Frontier Carbon Technology 15 (2005) 173–180.
[4] J.F.G. Oliveira, E.J. Silva, C. Guo, F. Hashimoto, Industrial challenges in grinding, CIRP Annals—Manufacturing Technology 58 (2009) 663–680.
[5] Y. Ichida, M. Fujimoto, Y. Inoue, K. Matsui, Development of a high performance vitrified grinding wheel using ultrafine-crystalline CBN abrasive grains, Advanced Mechanical Design Systems and Manufacturing 4 (2010) 1005–1014.
[6] H. Gao, Y.G. Zheng, W.G. Liu, J. Li, Development of vitrified bond CBN wheel for internal precision grinding of the air-conditioner compressor piston hole, Key Engineering Materials 304 (2006) 29–32.

[7] P. Beyer, High-production grinding with vitrified bond superabrasives—HPB technology for vitrified bond CBN wheels, Industrial Diamond Review 1 (2005) 46–48.
[8] D. Herman, J. Krzos, Influence of vitrified bond structure on radial wear of CBN grinding wheels, Journal of Materials Processing Technology 209 (2009) 5377–5386.
[9] J. Kopac, P. Krajnik, High-performance grinding—a review, Journal of Materials Processing Technology 175 (2006) 278–284.
[10] Y.G. Hou, G.Y. Qiao, Y. Shang, W.J. Zou, F.R. Xiao, B. Liao, Effect of porosity on the grinding performance of vitrified bond diamond wheels for grinding PCD blades, Ceramics International (2012), http://dx.doi.org/10.1016/j.ceramint.2012.04.074.
[11] T. Tanaka, S. Esaki, K. Nishida, T. Nakajima, K. Ueno, Development and application of porous vitrified-bonded wheel with ultra-fine diamond abrasives, Key Engineering Materials 257–258 (2004) 251–256.
[12] J. Webster, M. Tricard, Innovations in abrasive products for precision grinding, CIRP Annals—Manufacturing Technology 53 (2004) 597–617.
[13] B. Staniewicz-Brudnik, J. Plichta, K. Nadolny, Effect of porous glass–ceramic materials addition on the cubic boron nitride (CBN) tools properties, Optica Applicata 35 (2005) 809–817.
[14] M. Liu, B. Yu, J. Xu, J. Chen, Influence of pore formers on physical properties and microstructures of supporting cathodes of solid oxide electrolysis cells, International Journal of Hydrogen Energy 35 (2010) 2670–2674.
[15] M. Miyazaki, K. Sasaki, A. Suzuki, T. Terai, Microstructure control of Ni–ScSZ anode support for LT-SOFC, ECS Transactions 16 (2008) 67–81.
[16] T. Zeng, X. Dong, S. Chen, H. Yang, Processing and piezoelectric properties of porous PZT ceramics, Ceramics International 33 (2007) 395–399.
[17] K.H. Zuo, Y. Zhang, Y.P. Zeng, D.L. Jiang, Pore-forming agent induced microstructure evolution of freeze casted hydroxyapatite, Ceramics International 37 (2011) 407–410.
[18] M. Skovgaard, K.B. Andersen, K.K. Hansen, Pore former induced porosity in LSM/CGO cathodes for electrochemical cells for flue gas purification, Ceramics International 38 (2012) 1751–1754.
[19] M. Boaro, J.M. Vohs, R.J. Gorte, Synthesis of highly porous yttria-stabilized zirconia by tape-casting methods, Journal of the American Ceramic Society 86 (2003) 395–400.
[20] T. Zeng, X. Dong, C. Mao, Z. Zhou, H. Yang, Effects of pore shape and porosity on the properties of porous PZT 95/5 ceramics, Journal of the European Ceramic Society 27 (2007) 2025–2029.
[21] Y.F. Xia, Y.P. Zeng, D.L. Jiang, Mechanical and dielectric properties of porous Si_3N_4 ceramics using PMMA as pore former, Ceramics International 37 (2011) 3775–3779.
[22] C.H. Chen, S. Isiguro, S. Honda, H. Awaji, Homogenous alumina tube with controlled pore morphology, Materials Science and Engineering A 407 (2005) 167–173.
[23] C. Lian, Y. Zhuge, S. Beecham, The relationship between porosity and strength for porous concrete, Construction and Building Materials 25 (2011) 4294–4298.
[24] M.J. Jackson, B. Mills, Materials selection applied to vitrified alumina and CBN grinding wheels, Journal of Materials Processing Technology 108 (2000) 114–124.